Supporting Information

Development of Dual-responsive Fluorescent Probe for Drug Screening of Diabetes Cardiomyopathy

Ping-Zhao Liang, [a ‡] Zhe Li, [a ‡] Xing-Xing Zhang, [a] Fei-Yu Yang, [a] Su-Lai Liu, [b *] Tian-Bing Ren, [a] Lin Yuan, [a] and Xiao-Bing Zhang [a *]

a State Key Laboratory of Chemo/Biosensing and Chemometrics, College of Chemistry and Chemical Engineering, Hunan University, Changsha 410082, China

E-mail: xbzhang@hnu.edu.cn.

b Department of Hepatobiliary Surgery, Hunan Provincial People's Hospital/The First Affiliated Hospital of Hunan Normal University, Changsha, 410005, P. R. China

E-mail: liusulai@hunnu.edu.cn.

CONTENTS

1. Materials and Instruments

Materials and instruments. Unless otherwise stated, all reagents were purchased from commercial suppliers and used without further purification. **Lyso-Green**, **LC3B antibody**, **Horseradish peroxidase (HRP)-labeled secondary antibody**, **β-actin antibody,** and **Mdivi-1** were purchased from Beyotime. **Drp-1 antibody** was purchased from Absin Biotechnology. **Mito-blue** was synthesized based on reported literature. [1] **N-Acetyl-L-cysteine (NAC)**, **Luteolin (Lut)**, **Taxifolin (TAX)**, **Resveratrol (Res)**, **Icariin (ICA)**, **Curcumin (Cur),** and **Rutinum (Rut)** were purchased from Macklin. Solvents were purified by standard methods prior to use. Twice-distilled water was used throughout all experiments. Mass spectra were performed using an Agilent 1200-6520 Q-TOF mass spectrometer system operating in a MALDI-TOF mode. NMR spectra were recorded on Bruker-400, using TMS as the internal standard. UV–vis spectra were recorded on a UV-1800 spectrophotometer (Shimadzu Corporation, Japan). One-photon photoluminescence spectra were recorded on a HITACHI F4600 fluorescence spectrophotometer with a 1 cm standard quartz cell. Cell imaging was performed on Nikon A1plus confocal microscope. The pH measurements were carried out on a PHS-3C pH meter (INESA instrument). TLC analysis was performed on silica gel plates and column chromatography was conducted over silica gel (mesh 200–300) columns, obtained from the Yantai Jiangyou silica gel Development Company Limited.

2. Synthesis of Compounds and response mechanism of HDB

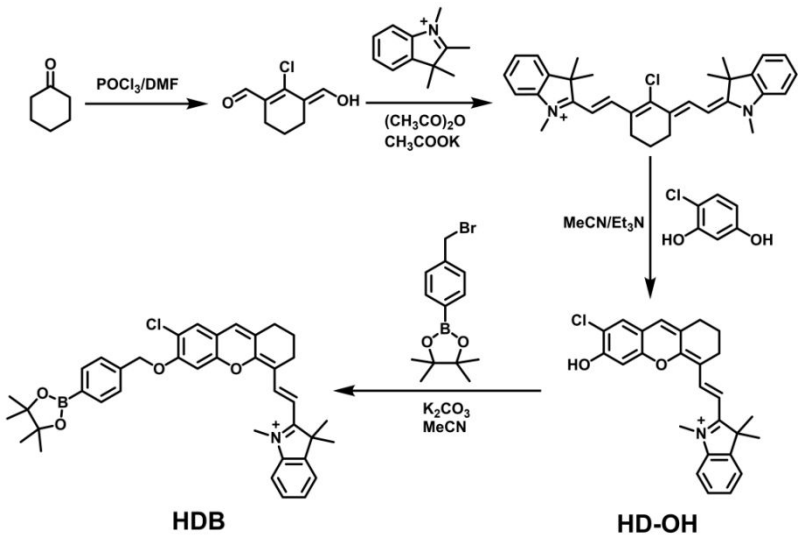

Scheme S1 The synthetic route of **HDB**.

Synthesis of Compound HDB. HD-OH was synthesized according to reported procedures. 2-(4-Bromobenzyl)-4,4,5,5-tetramethyl-1,3,2-dioxaborolane (163 mg, 0.55 mmol), **HD-OH** (100 mg, 0.183 mmol) and K_2CO_3 (75.9 mg, 0.55 mmol) were dissolved in MeCN. The mixture was

stirred at 70 ℃ under a nitrogen atmosphere. After 4 h, the solvent was removed under reduced pressure. And the residue was subjected to silica gel chromatography, and eluted with CH_2Cl_2/MeOH (v/v, 30:1), to afford compound **HDB** as a blue solid (60.5 mg, yield 52.1 %). ^{1}H NMR (400 MHz, MeOD-d_4) δ 8.73 (d, J = 13.7 Hz, 1H), 7.83 (s, 1H), 7.71(d, J = 6 Hz, 2H), 7.60 (t, J = 2.7 Hz, 3H), 7.54 (m, 3H), 7.26 (m, 2H), 6.57 (d, J = 15.0 Hz, 1H), 5.41 (s, 2H), 3.91 (s, 3H), 2.72-2.80 (m, 4H), 1.95 (t, J = 6.2 Hz, 2H), 1.84 (s, 6H), 1.35-1.30 (s, 12H). ^{13}C NMR (100 MHz, MeOD-d_4) δ 179.69, 162.06, 157.92, 147.17, 144.15, 142.67, 133.75, 132.20, 129.39, 128.83, 128.46, 128.06, 127.68, 126.87, 126.58, 125.95, 121.81, 119.70, 116.68, 115.20, 112.63, 106.28, 101.15, 70.10, 51.63, 51.35, 37.58, 35.75, 35.13, 34.56, 31.60, 28.94, 28.31, 27.39, 25.92, 25.52, 23.61, 22.97, 20.13, 14.61, 13.05. MS (MALDI-TOF): calcd for $C_{39}H_{42}BClNO_4^+$ M^+ 634.29, found 634.32.

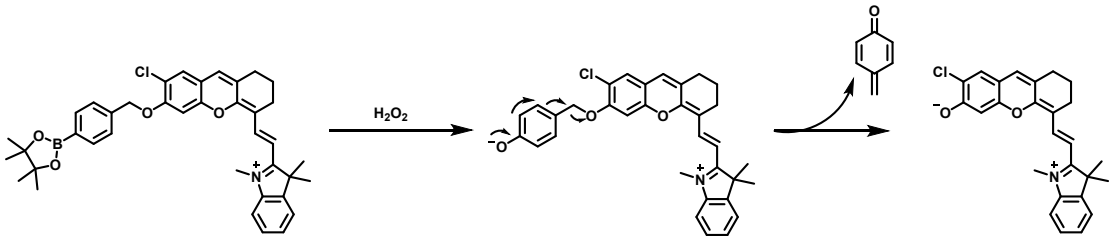

Scheme S2 Recognition mechanism of **HDB** toward H_2O_2.

3. Spectral Measurements

The fluorescence measurement experiments were measured in PBS (10 mM, pH = 7.4) with EtOH as co-solvent solution (PBS/ EtOH = 8:2, v/v). For the **HDB**, a volume of 5 μL of **HDB** stock solution (1 mM), 20 μL of H_2O_2 solution (10 mM), and PBS buffer solution were added into a tube to make the final volume 1 mL. After incubation at 37 °C for 30 min, the reaction solution was transferred into a quartz cell to measure the absorbance or fluorescence spectra, with both excitation and emission slits set at 10 nm. Different pH values of PBS solution from 3. 0 to 8.5 was adjusted by adding minimal volumes of HCl solution or NaOH solution. The solutions of various testing species were prepared preliminary by using twice-distilled water with the final interference concentration: Cys (100 μM); GSH (100 μM); H_2O_2 (100 μM); H_2S (100 μM); HClO (10 μM); HSO_3^- (100 μM); NO_3^- (100 μM); $O_2^{\cdot-}$ (50 μM); $ONOO^-$ (10 μM). The fluorescence spectra were measured with excitation wavelength at 560 nm.

4. Cell Imaging and analysis

When the cell density reached 90% of confluence, a subculture was done and the medium was changed approximately every day. Cells were first seeded in a 20 mm glass-bottom dish plated and grown to around 80% confluency for 24 h before the experiment. When incubating H9C2 cells, both high glucose medium and low glucose medium were prepared from a sugar-free DMEM medium. The high glucose medium contained 30 mM glucose and the normal glucose medium contained 5 mM glucose, and the osmolality was adjusted with mannitol to coincide with

the high glucose medium. Fluorescence imaging of cells was carried out using the Nikon A1plus confocal microscope with a 60× oil immersion objective lens. The fluorescence signal of cells incubated with **HDB** was collected at 663-738 nm and the fluorescence signal of **HD-OH** was collected in the green channel (584-676 nm) and red channel (735-750 nm) by using the semiconductor laser at 561 nm as excitation resource. To quantify the fluorescence intensity in cells, open-source image analysis software (ImageJ, NIH) was used.

5. Cytotoxicity Assays

Cytotoxicity assays were carried out using HeLa cells and H9C2 cells. Cell viability was determined using the MTT assay. 8000 cells per well were seeded in a 96-well plate and incubated for 12 h in a humidified incubator for adherence. **HDB** dissolved in DMSO was added to cells at the final concentration of 0, 5, 10, 15, and 20 μM and incubated for 24 h. MTT reagent diluted by DMEM medium (10%) was added to each well after the removal of culture media and incubated for 0.5 h. Following that, the absorbance was measured at 490 nm on a plate reader Synergy 2 Multi-Mode Microplate Reader (Bio-Tek, Winooski, VT).

6. Western blot analysis.

The cells were washed 3 times with DPBS, scraped off with a cell scraper, and the cell proteins were extracted strictly according to the instructions of the protein extraction kit and then subjected to polypropylene gel electrophoresis (8% separation gel, 5% concentrated gel). The upper gel electrophoresis was performed at 80 V, and the lower gel electrophoresis was performed at 120 V for 2 h. Then, the proteins were transferred to the PVDF membrane by wet transfer (300 mA constant current, 2 h). After the membranes were blocked in 5% skimmed milk in Tris-buffered saline Tween-20 (TBS-T) for 2 h at room temperature, they were incubated with β-actin antibodies at 1/1000 or Drp-1 antibodies at a 1/1000 dilution overnight at 4℃. After three washes, the horseradish peroxidase (HRP)-coupled secondary antibody was added and incubated at room temperature for 1 h. Finally, the bands were detected by a chemiluminescence kit. For quantifying protein expression, open-source image analysis software (ImageJ, NIH) was used.

7. Additional experiments

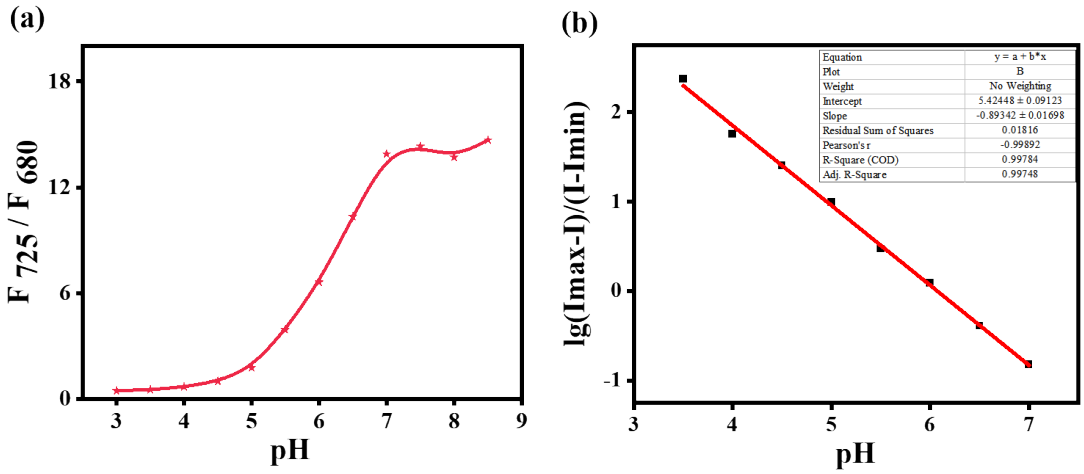

Figure S1. (a) Plots of F_{725} / F_{680} versus pH for **HD-OH** (5 μM). (b) The linear relationship between lg [(I max - I)/ (I - I min)] and pH (3.5 - 6.5). The pKa value was calculated using the Henderson–Hasselbalch equation: lg [(I max - I)/ (I - I min)] = pH - p*Ka*. [2] Slit width: d_{ex}= d_{em}= 10 nm.

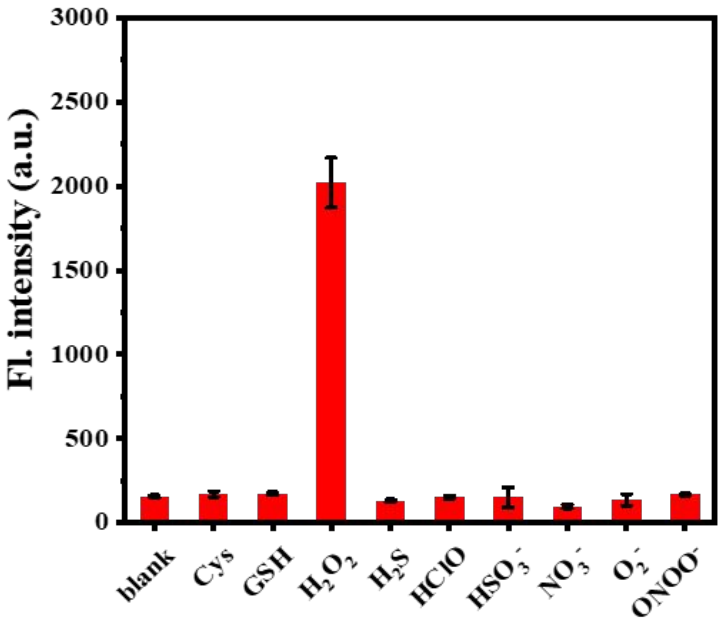

Figure S2. Fluorescence intensity (at 725 nm) of **HDB** (5 μM) with excitation at 640 nm in the presence of various species: blank; Cys (100 μM); GSH (100 μM); H_2O_2 (100 μM); H_2S (100 μM); HClO (10 μM); HSO_3^- (100 μM); NO_3^- (100 μM); $O_2^{\cdot-}$ (50 μM); $ONOO^-$ (10 μM). All species were shaken with **HDB** at 37°C for 1 h before testing. Slit width: d_{ex}= d_{em}= 10 nm.

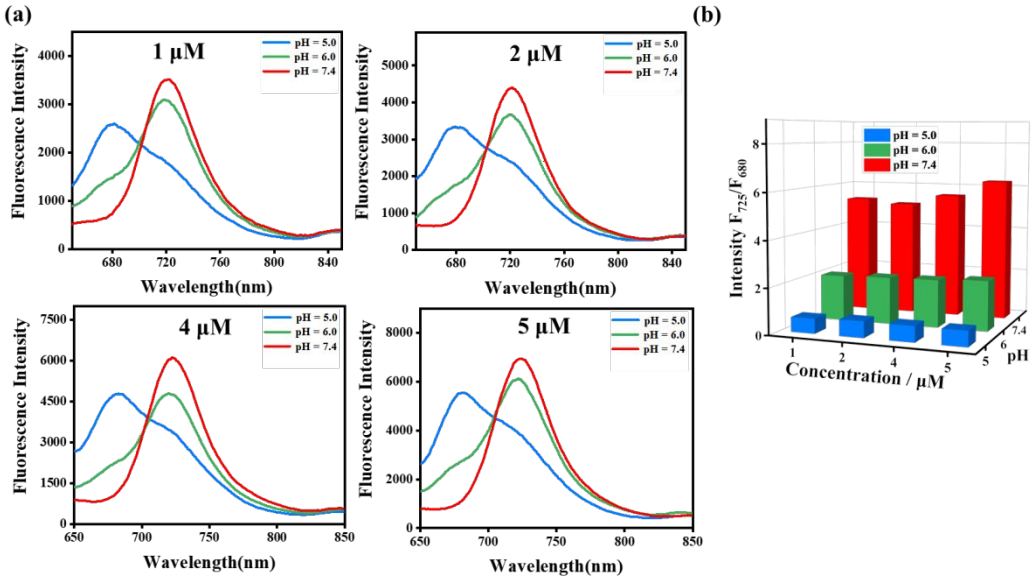

Figure S3. (a) Changes of **HD-OH** fluorescence at different concentrations (1 μM, 2 μM, 4 μM, 5 μM) in buffer solutions of different pH (PBS: EtOH = 8:2, pH = 5.0, 6.0, 7.4). λ_{ex} = 560 nm. (b) Normalized analysis of the ratiometric fluorescence change (F_{725}/F_{680}) in a. Slit width: d_{ex}= d_{em}= 10 nm.

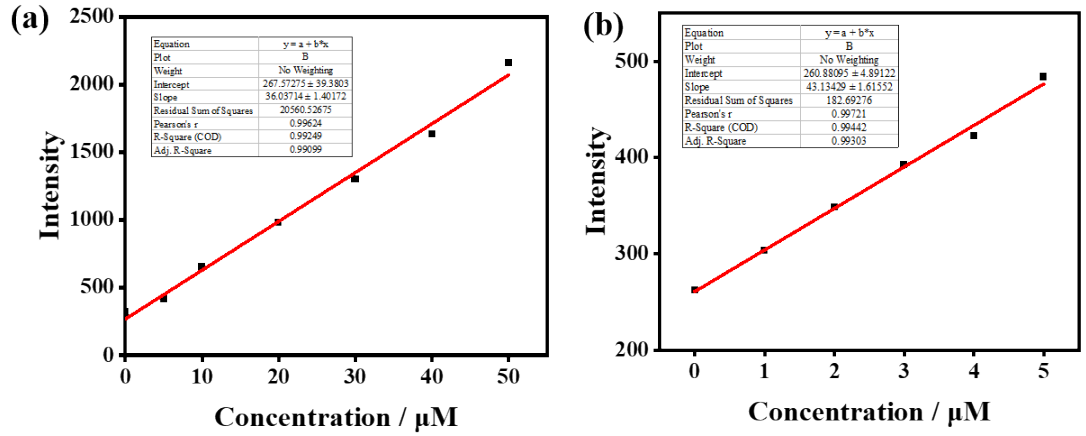

Figure S4. The detection limit was calculated based on the fluorescence titration of **HDB** (5 μM) in the presence of H_2O_2. Fluorescence spectra of **HDB** (5 μM) in PBS buffer solution (10 mM, pH=7.4, PBS: EtOH = 8:2) upon addition of H_2O_2 shaken at 37°C with 1h. (a) Concentration range: 0 - 50 μM. (b) Concentration range: 0 - 5 μM. The fluorescence intensity of **HDB** was measured by three times, and standard deviation of the blank measurement was achieved. The detection limit was calculated by the following equation: detection limit = 3σ/ k, where σ is the standard deviation of the blank measurement and k is the slope between the fluorescence emission intensity (I = 725 nm) versus different H_2O_2 concentrations. λ_{ex} = 640 nm. Slit width: d_{ex}= d_{em}= 10 nm.

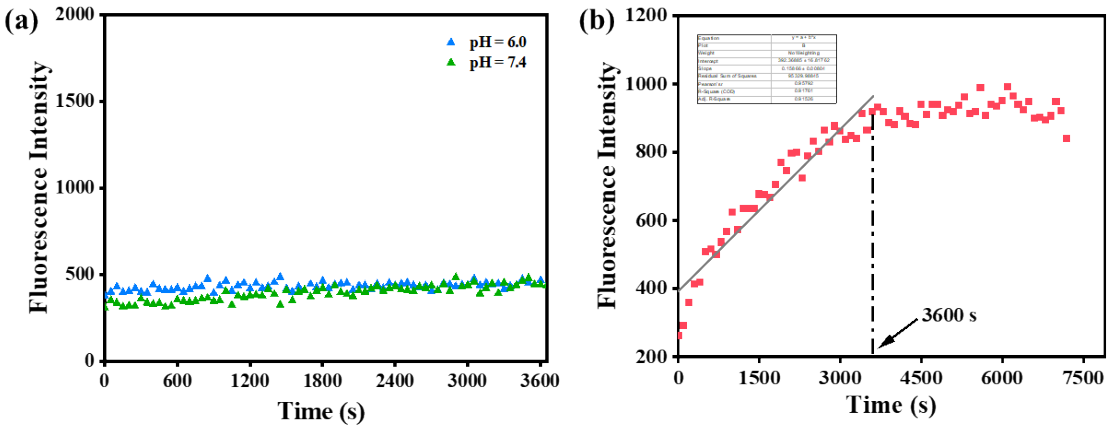

Figure S5. A plot of the fluorescence intensity of **HDB** (5 μM) vs. reaction time at 37 ℃ (PBS: EtOH = 8:2). (a) Blue curve: Time scan of fluorescence intensity of **HDB** (5 μM) collected at 725 nm at pH 6.0. Green curve: Time scan of fluorescence intensity of **HDB** (5 μM) collected at 725 nm at pH 7.4. (b) Time scan of the fluorescence intensity of **HDB** (5 μM) collected at 725 nm in the presence of 50 μM H_2O_2. λ_{ex} = 640 nm. Slit width: d_{ex}= d_{em}= 10 nm.

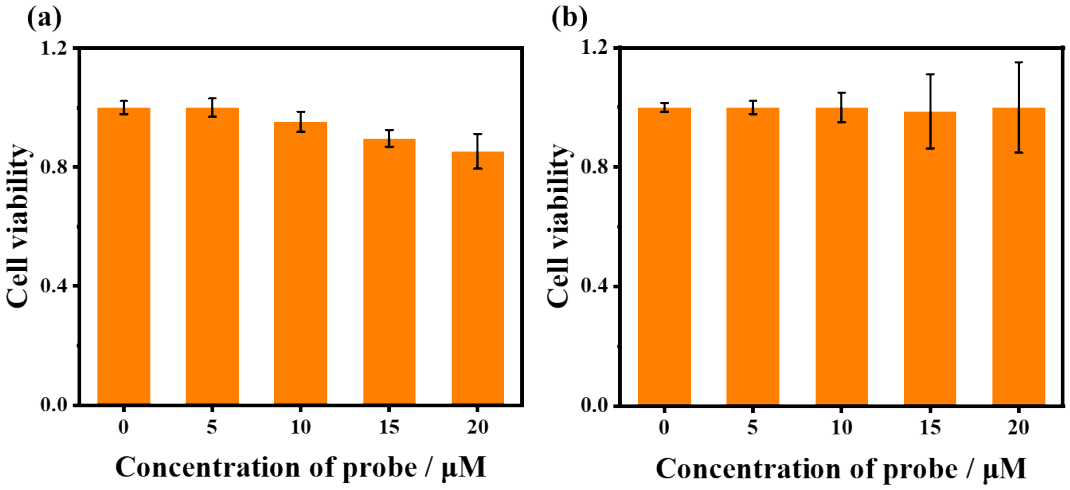

Figure S6. Cell viability of (a) H9C2 cells. (b) Hela cells were treated with different concentrations of **HDB** for 24 h in the fresh medium. The results are the mean standard deviation of four separate measurements.

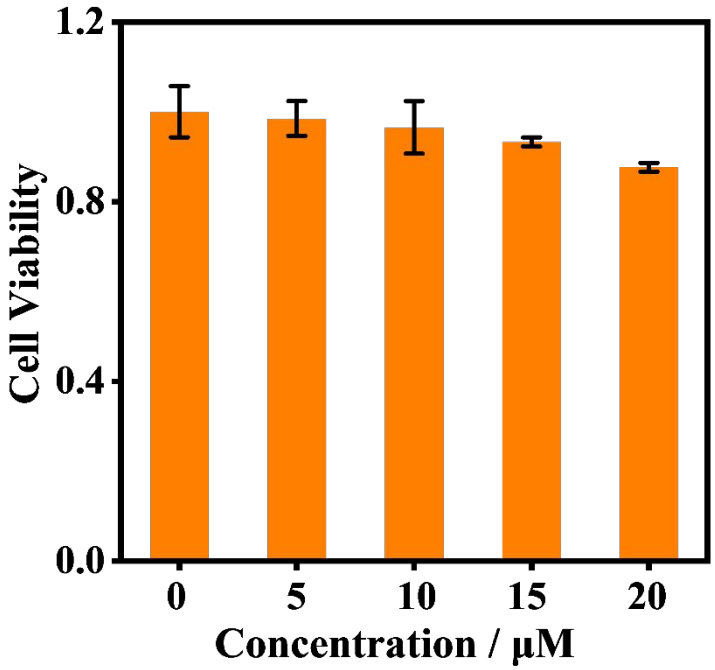

Figure S7. Cell viability of Hela cells were treated with different concentrations of **HD-OH** for 24 h in the fresh medium. The results are the mean standard deviation of four separate measurements.

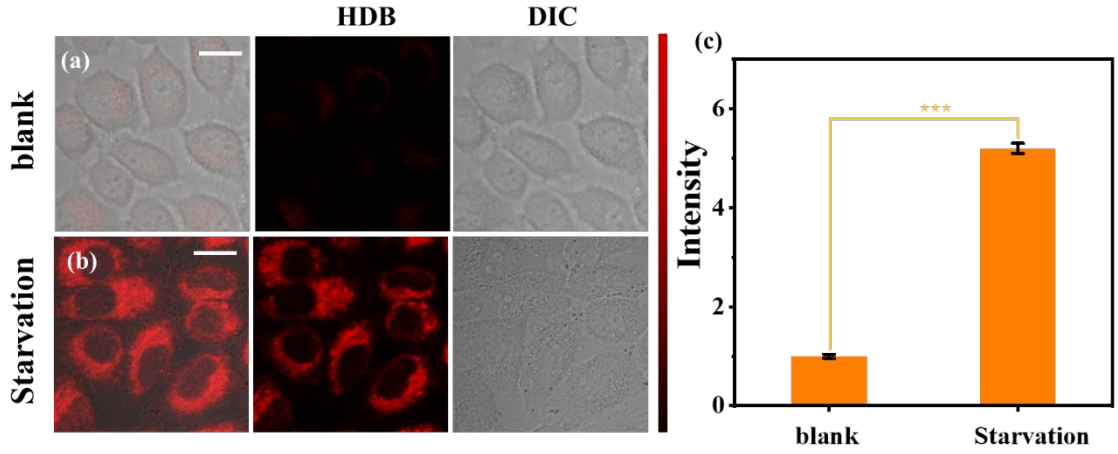

Figure S8. Real-time imaging of HeLa cells incubated with (a) **HDB** (10 μM) (Hela cells were cultured with normal medium for 4 h, and then **HDB** was added for 1 h). (b) **HDB** (10 μM) (Hela cells were cultured with serum-free medium for 4h, and then **HDB** was added for 1 h). λ_{em} = 663-738 nm, λ_{ex} = 561 nm. Scale bar: 20 μm. (c) The histogram: normalized average fluorescence intensity of **HDB** in a and b. Error bars, ± s. e. m. n = 3. ***p < 0.001.

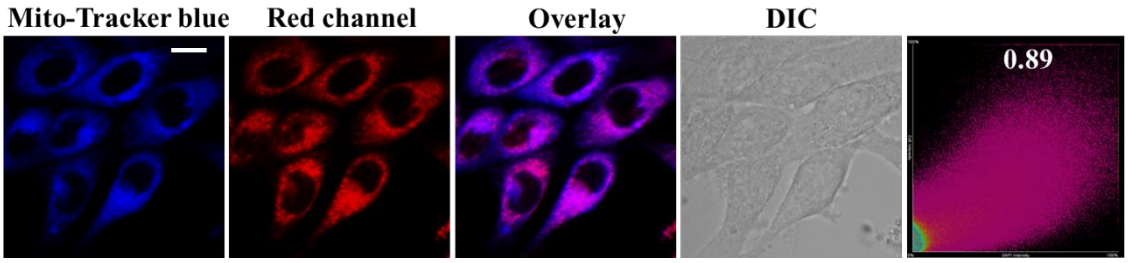

Figure S9. Mitochondrial co-localization in Hela cells. Hela cells were co-incubated with **HD-OH** (10 μM) and Mito-Tracker blue (5 μM) for 30 min. Red channel: λ_{em} = 663 - 738 nm, λ_{ex} = 561 nm. Mito-Tracker blue channel: λ_{em} = 425 - 475 nm, λ_{ex} = 405 nm. Scale bar: 20 μm.

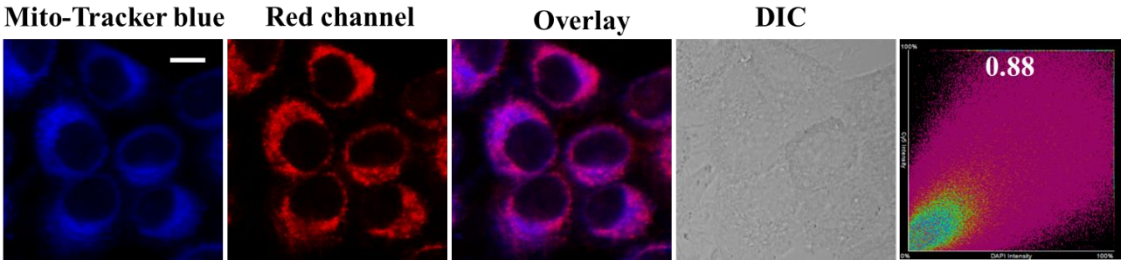

Figure S10. Mitochondrial co-localization in Hela cells after starvation induction. Hela cells were incubated in serum-free DMEM medium for 4 h and then co-incubated with **HDB** (10 μM) and Mito-Tracker blue (5 μM) for 30 min. Red channel: λ_{em} = 663 - 738 nm, λ_{ex} = 561 nm. Mito-Tracker blue channel: λ_{em} = 425 - 475 nm, λ_{ex} = 405 nm. Scale bar: 20 μm.

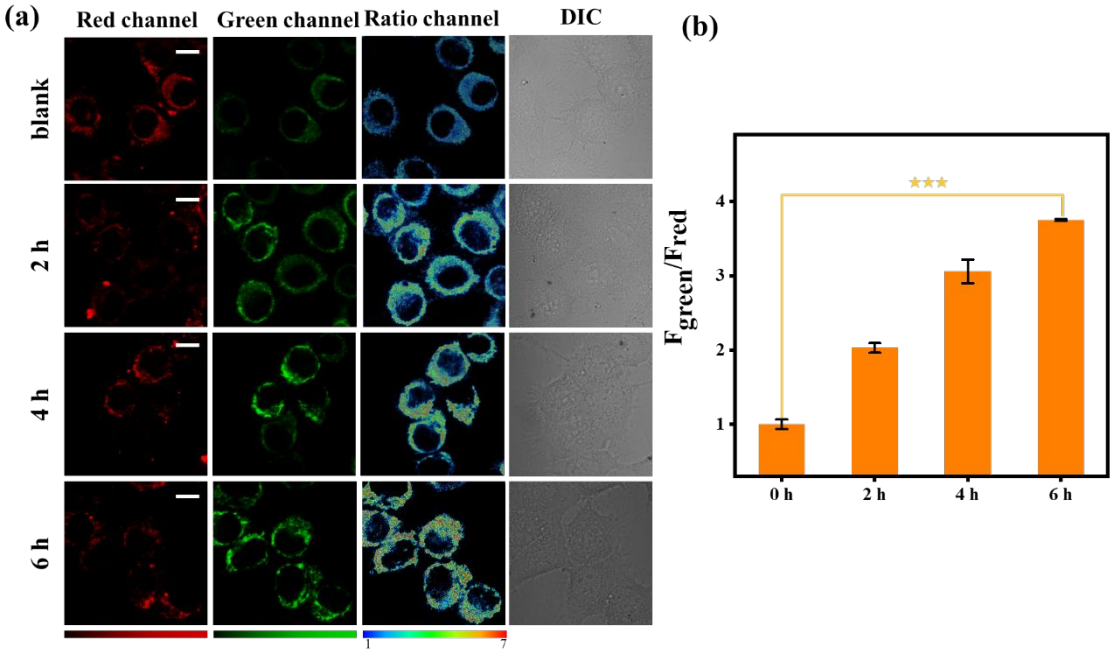

Figure S11. Real-time tracking of hunger-induced mitophagy in HeLa cells at different time points. (a) Fluorescence imaging of HeLa cells with **HDB** (10 μM) for 1 h and cells was incubated by normal DMEM media or serum-free DMEM media for 2 h, 4 h, and 6 h. Green channel: λ_{em} = 584-676 nm, red channel: λ_{em} = 735 - 750 nm, λ_{ex} = 561 nm. Scale bar: 20 μm. (b) The histogram:

the ratio (F_{green}/F_{red}) at different times, F_{green} and F_{red}: the fluorescence intensity of green and red channels, respectively. Error bars, ± s. e. m. n = 3. ***p < 0.001.

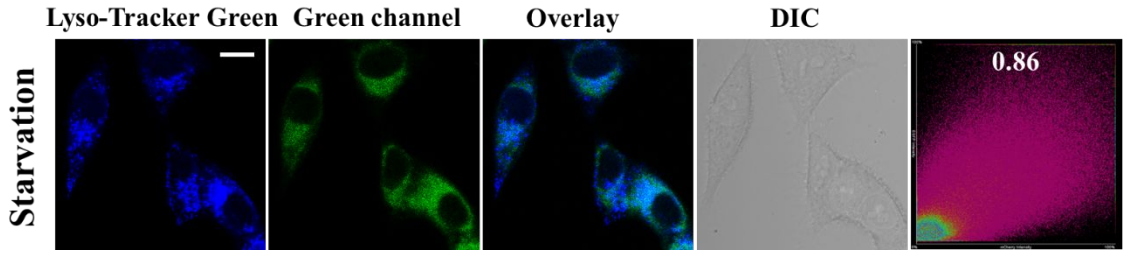

Figure S12. Co-localization during starvation-induced mitophagy in Hela cells. Hela cells were incubated for 4 h with serum-free medium. The group was incubated with **HDB** (10 μM) for 30 min and Lyso-Tracker green (1 μM) for 10 min. Green channel: λ_{em} = 584 - 676 nm, λ_{ex} = 561 nm. Lyso-Tracker green channel: λ_{em} = 500 - 550 nm, λ_{ex} = 488 nm. Scale bar: 20 μm.

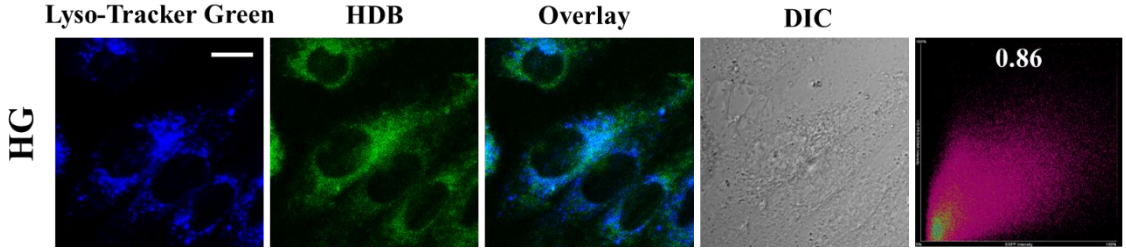

Figure S13. Co-localization experiments of H9C2 cells incubated in DMEM medium with high glucose (30 mM). The group was incubated with **HDB** (10 μM) for 30 min and Lyso-Tracker green (1 μM) for 10 min. Green channel: λ_{em} = 584 - 676 nm, λ_{ex} = 561 nm. Lyso-Tracker green channel: λ_{em} = 500 - 550 nm, λ_{ex} = 488 nm. Scale bar: 20 μm.

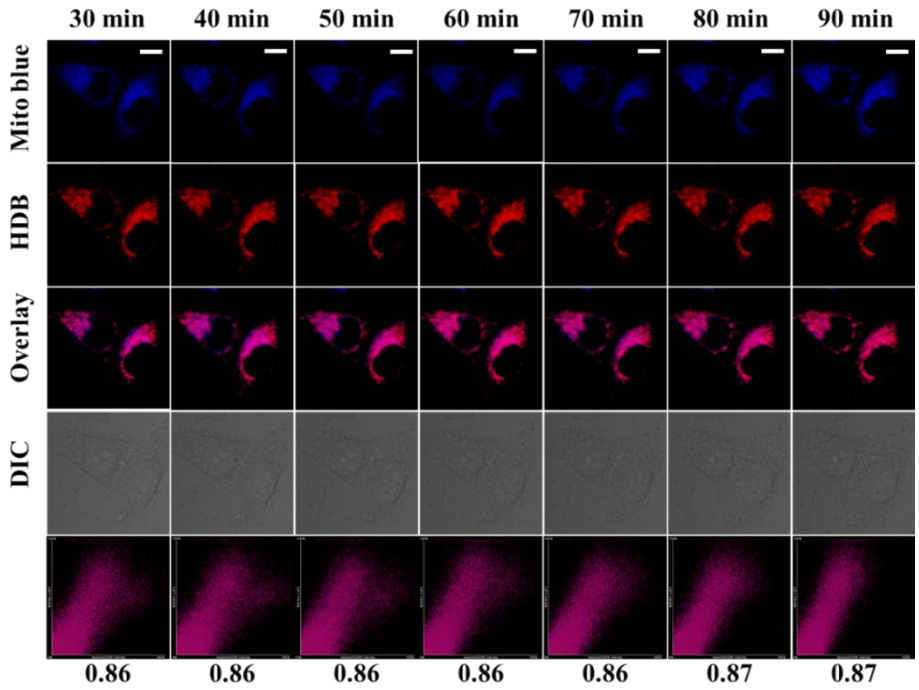

Figure S14. Fluorescence images of HeLa cells incubated with **HDB** (10 μM) for different times in the presence of H_2O_2 (300 μM). Mito-Tracker Blue channel: λ_{ex} = 405 nm, λ_{em} = 425 - 475 nm. **HDB** channel: λ_{ex} = 561 nm, λ_{em} = 663 - 738 nm. Scale bar: 20 μm.

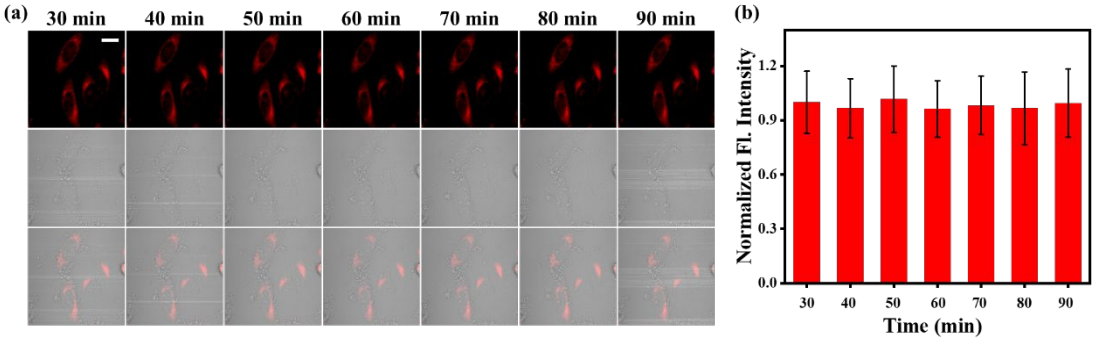

Figure S15 (a) Fluorescence imaging of **HDB** (10 μM) in high-glucose incubated H9C2 cells at different time points. Red channel: λ_{ex} = 640 nm, λ_{em} = 663-738 nm. Scale bar: 20 μm. (b) Normalized fluorescence intensity of the red channel in Figure a.

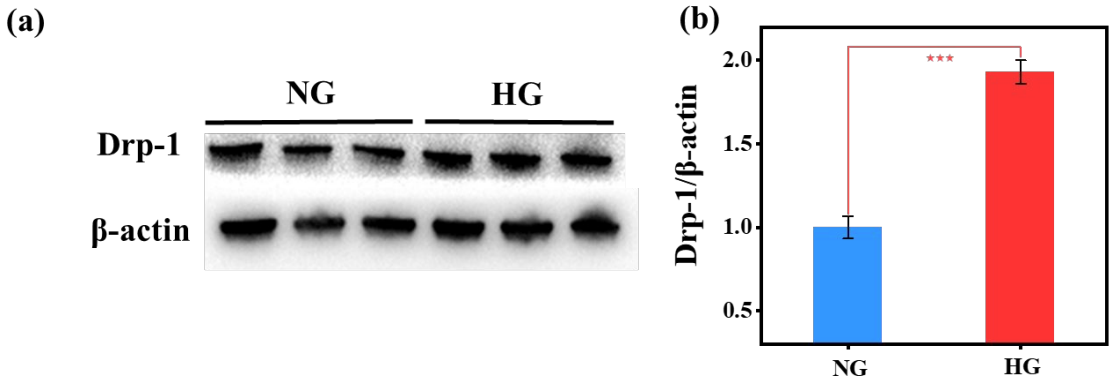

Figure S16. (a) H9C2 cells were incubated in low (5 mM glucose) or high glucose (30 mM glucose) conditions for 24 h. Total cell extracts were analyzed by western blotting with antibodies against Drp-1. Western blot of β-actin was used as a loading control. (b) Image J normalized quantitative analysis of the Drp-1/β-actin ratios from western blot in a. Error bars, ± s. e. m. n = 3. ***$p < 0.001$.

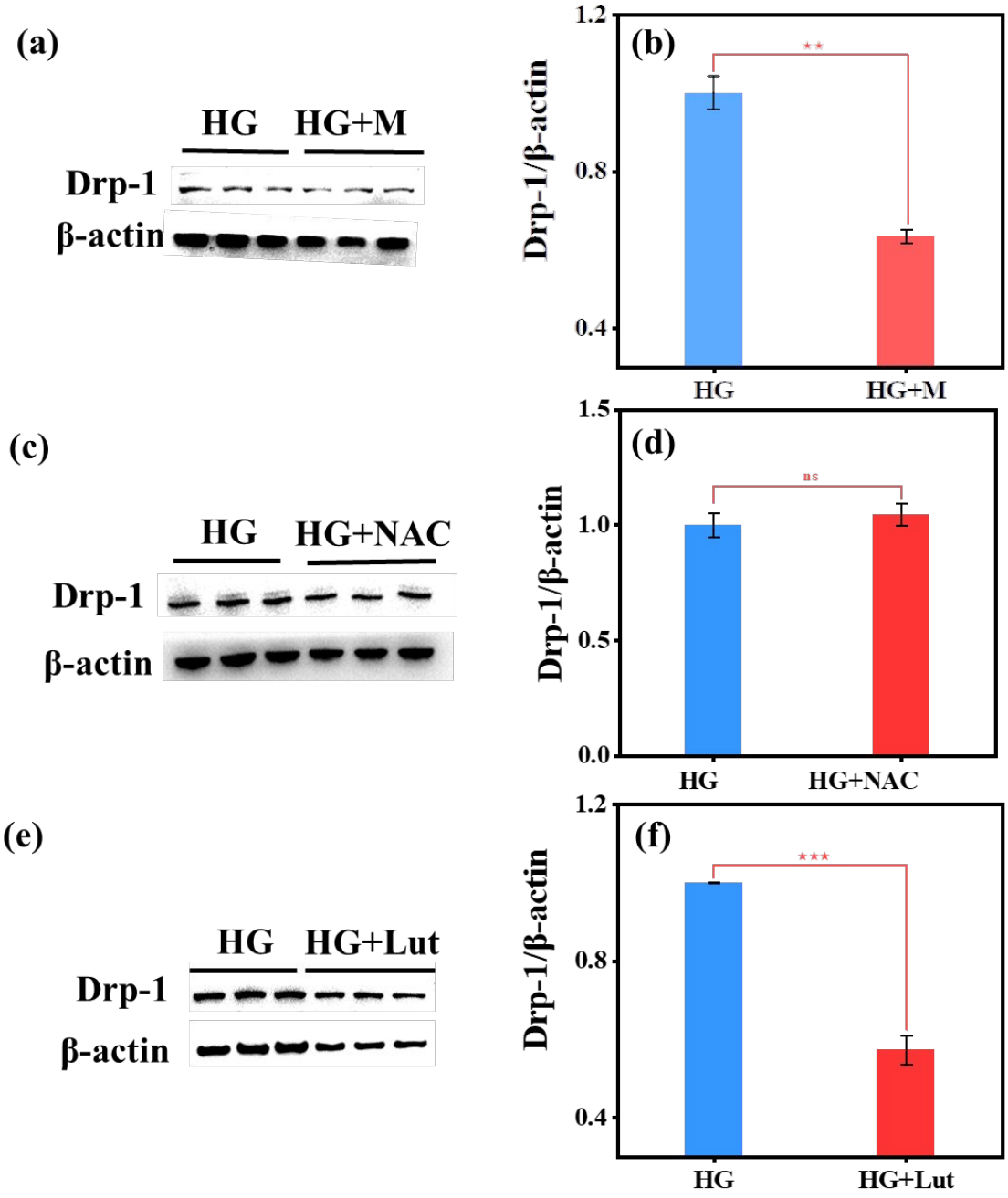

Figure S17. The total cell extracts were analyzed using western blotting with antibodies against Drp-1. (a): High glucose (30 mM) and Mdivi-1 (5 μM) were used to co-culture cells for 2 h. (b) Image J normalized quantitative analysis of the Drp-1/β-actin ratios from immunoblots in a. (c): High glucose (30 mM) and NAC (100 μM) were used to co-culture cells for 2 h. (d) Image J normalized quantitative analysis of the Drp-1/β-actin ratios from immunoblots in c. (e): High glucose (30 mM) and Lut (50 μM) were used to co-culture cells for 2 h. (f) Image J normalized quantitative analysis of the Drp-1/β-actin ratios from immunoblots in e. Error bars, ± s. e. m. n = 3. **$p < 0.01$. ***$p < 0.001$.

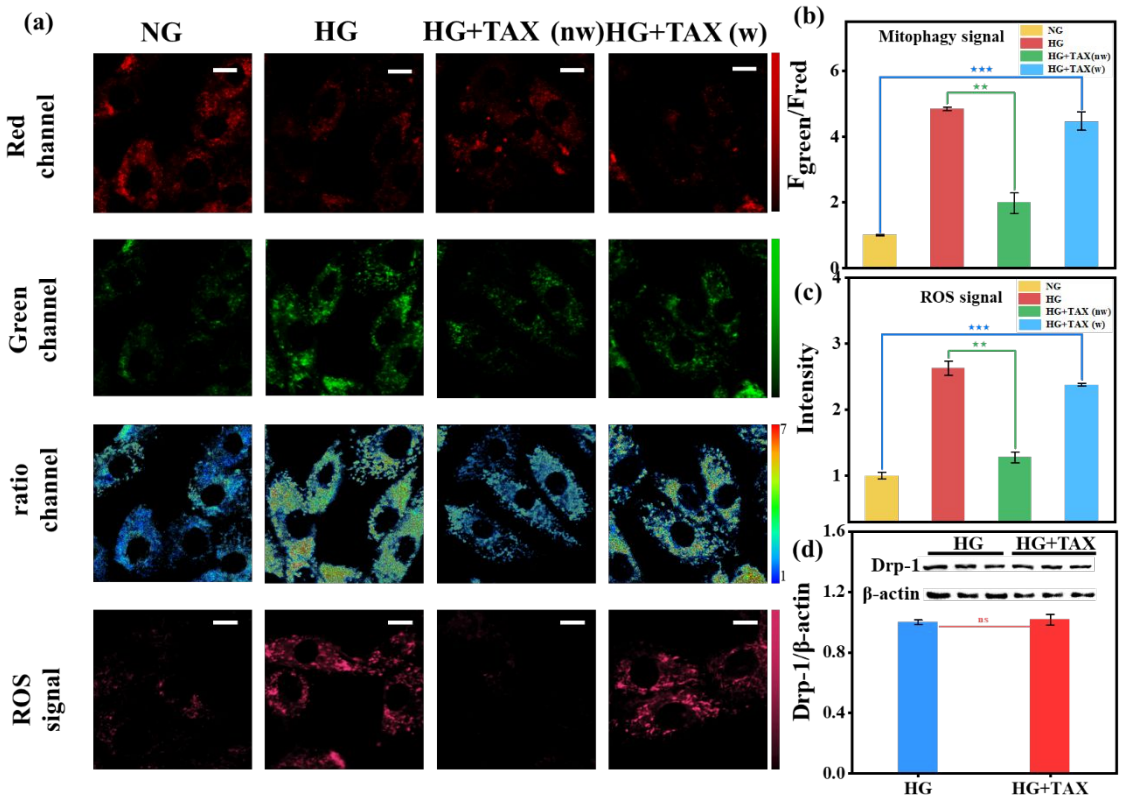

Figure S18. Real-time fluorescence imaging of H9C2 incubated with **HDB** (10 μM). (a) H9C2 cells were incubated with **HDB** under different conditions. NG: Normal group (5 mM glucose). HG: DCM group (30 mM glucose). HG+TAX (w): high-glucose-cultured H9C2 cells were incubated with TAX (200 μM) for 1 h, then, washed off TAX and incubated with **HDB** for another hour. HG+TAX (nw): high-glucose-cultured H9C2 cells were incubated for one hour with TAX (200 μM) and then incubated for another hour with **HDB** without washing off the TAX. (b) Normalized average fluorescence intensity of the ratio channel in a. Green channel: λ_{em} = 584 - 676 nm, red channel: λ_{em} = 735 - 750 nm, λ_{ex} = 561 nm. Scale bar: 20 μm. (c) Normalized average fluorescence intensity of the ROS level in a. ROS level: λ_{em} = 663 - 738 nm, λ_{ex} = 561 nm. Scale bar: 20 μm. (d) H9C2 cells were incubated with high glucose for 24 h and then incubated with TAX (200 μM) for 4 h. (d) Image J normalized quantitative analysis of the Drp-1/β-actin ratios from immunoblots. Inset: Western blot analysis of Drp-1 in HG and HG+TAX groups. As shown by the fluorescence images, both the mitophagy signal and ROS signal were inhibited in the no-wash group, while the two signals in the wash-off group were not significant compared with the HG control group, which indicated that TAX was an antioxidant drug. Meanwhile, WB experiments also showed that the Drp-1 content was unchanged after adding the drug for 2 h. Error bars, ± s. e. m. n = 3. **p < 0.01 and ***p < 0.001. Bright field image of cell imaging: Figure S28.

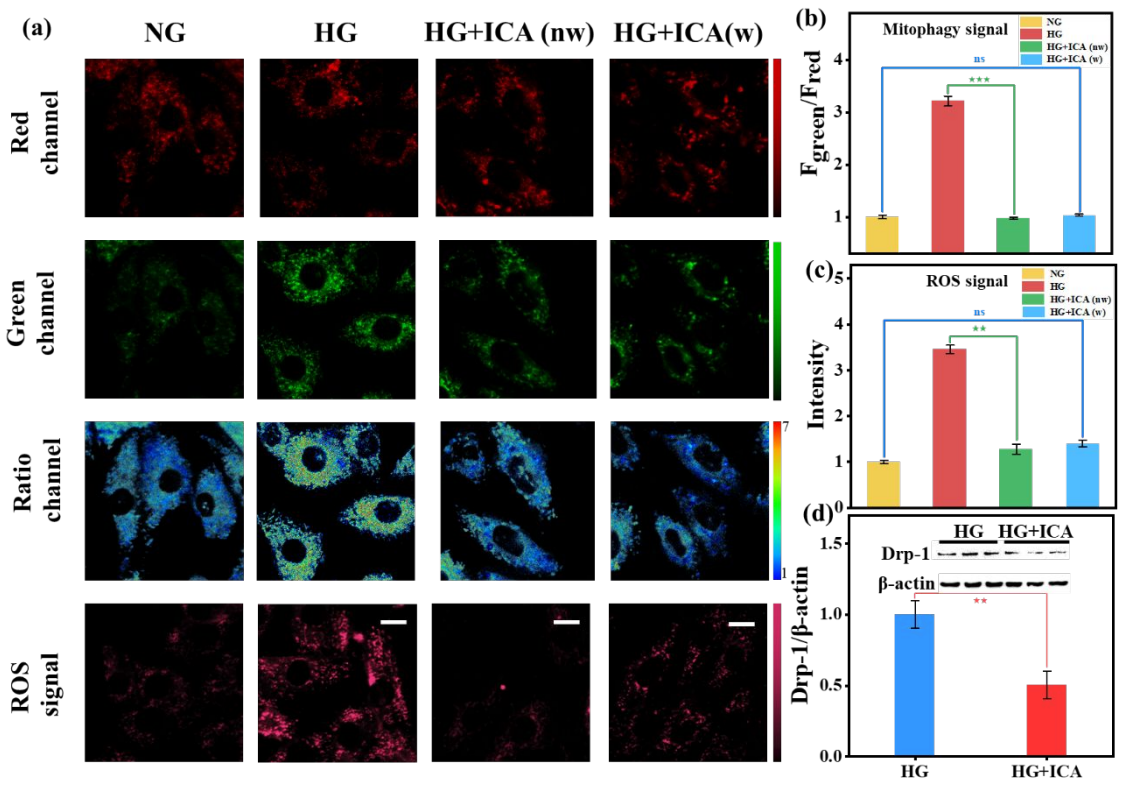

Figure S19. Real-time fluorescence imaging of H9C2 incubated with **HDB** (10 μM). (a) H9C2 cells were incubated with **HDB** under different conditions. NG: Normal group (5 mM glucose). HG: DCM group (30 mM glucose). HG+ICA (w): high-glucose-cultured H9C2 cells were incubated with ICA (10 μM) for 1 h, then, washed off ICA and incubated with **HDB** for another hour. HG+ICA (nw): high-glucose-cultured H9C2 cells were incubated for one hour with ICA (10 μM) and then incubated for another hour with **HDB** without washing off the ICA. (b) Normalized average fluorescence intensity of the ratio channel in a. Green channel: λ_{em} = 584 - 676 nm, red channel: λ_{em} = 735 - 750 nm, λ_{ex} = 561 nm. Scale bar: 20 μm. (c) Normalized average fluorescence intensity of the ROS level in a. ROS level: λ_{em} = 663 - 738 nm, λ_{ex} = 561 nm. Scale bar: 20 μm. (d) H9C2 cells were incubated with high glucose for 24 h and then incubated with ICA (10 μM) for 4 h. (d) Image J normalized quantitative analysis of the Drp-1/β-actin ratios from immunoblots. Inset: Western blot analysis of Drp-1 in HG and HG+ICA groups. As shown by the fluorescence images, the mitophagy signal and ROS signal were inhibited in both the wash-off and no-wash groups compared to the HG control group, which indicated that ICA was a dual-effect drug. Meanwhile, WB experiments also showed that Drp-1 expression could be effectively inhibited after adding the drug for 2 h. Error bars, ± s. e. m. n = 3. **p < 0.01 and ***p < 0.001. Bright field image of cell imaging: Figure S28.

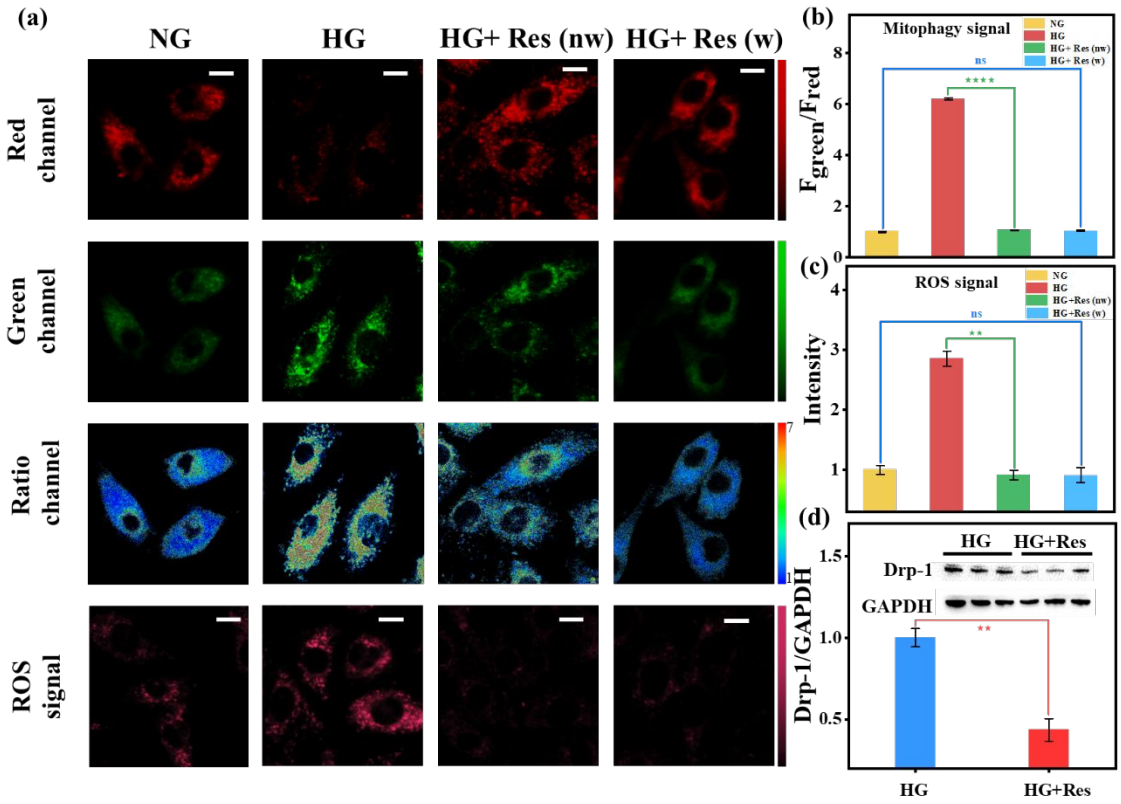

Figure S20. Real-time fluorescence imaging of H9C2 incubated with **HDB** (10 μM). (a) H9C2 cells were incubated with **HDB** under different conditions. NG: Normal group (5 mM glucose). HG: DCM group (30 mM glucose). HG+Res (w): high-glucose-cultured H9C2 cells were incubated with Res (200 μM) for 1 h, then, washed off Res and incubated with **HDB** for another hour. HG+ Res (nw): high-glucose-cultured H9C2 cells were incubated for one hour with Res (200 μM) and then incubated for another hour with **HDB** without washing off the Res. (b) Normalized average fluorescence intensity of the ratio channel in a. Green channel: λ_{em} = 584 - 676 nm, red channel: λ_{em} = 735 - 750 nm, λ_{ex} = 561 nm. Scale bar: 20 μm. (c) Normalized average fluorescence intensity of the ROS level in a. ROS signaling: λ_{em} = 663 - 738 nm, λ_{ex} = 561 nm. Scale bar: 20 μm. (d) H9C2 cells were incubated with high glucose for 24 h and then incubated with Res (200 μM) for 4 h. (d) Image J normalized quantitative analysis of the Drp-1/GAPDH ratios from immunoblots. Inset: Western blot analysis of Drp-1 in HG and HG+Res groups. As shown by the fluorescence images, the mitophagy signal and ROS signal were inhibited in both the wash-off and no-wash groups compared to the HG control group, which indicated that Res was a dual-effect drug. Meanwhile, WB experiments also showed that Drp-1 expression could be effectively inhibited after adding the drug for 2 h. Error bars, ± s. e. m. n = 3. **p < 0.01 and ****p < 0.0001. Bright field image of cell imaging: Figure S28.

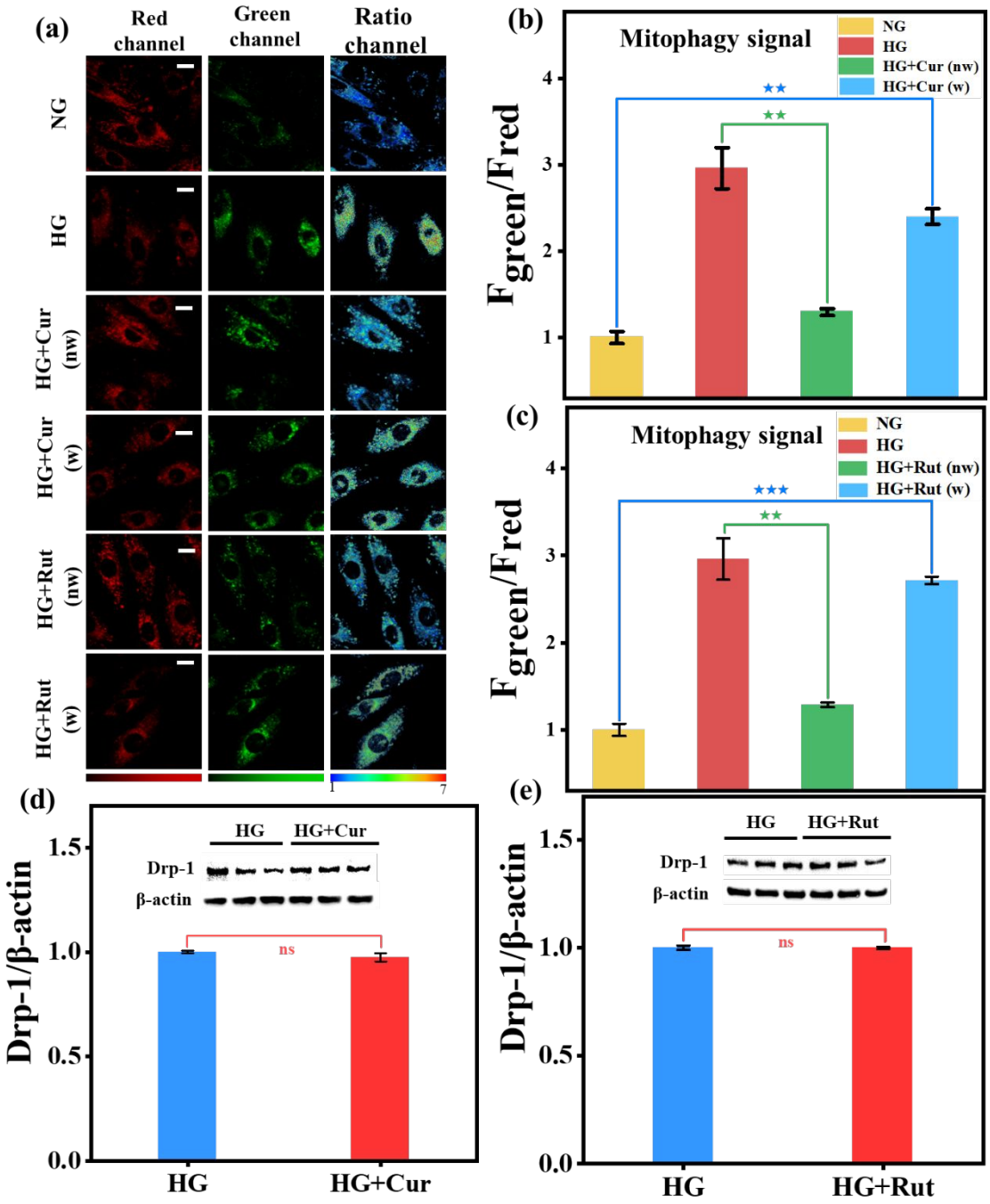

Figure S21. Real-time fluorescence imaging of H9C2 incubated with **HDB** (10 μM). (a) H9C2 cells were incubated with **HDB** under different conditions. NG: Normal group (5 mM glucose). HG: DCM group (30 mM glucose). HG+Cur (w): high-glucose-cultured H9C2 cells were incubated with Cur (30 μM) for 1 h, then, washed off Cur and incubated with **HDB** for another hour. HG+Cur (nw): high-glucose-cultured H9C2 cells were incubated for one hour with Cur (30 μM) and then incubated for another hour with **HDB** without washing off the Cur. HG+Rut (w): high-glucose-cultured H9C2 cells were incubated with Rut (40 μM) for 1 h, then, washed off Rut and incubated with **HDB** for another hour. HG+ Rut (nw): high-glucose-cultured H9C2 cells were incubated for one hour with Rut (40 μM) and then incubated for another hour with **HDB** without washing off the Rut. Green channel: λ_{em} = 584 - 676 nm, red channel: λ_{em} = 735 - 750 nm, λ_{ex} = 561 nm. Scale bar: 20 μm. (b-c) Normalized average fluorescence intensity of the ratio channel in

a. (d-e) Image J normalized quantitative analysis of the Drp-1/β-actin ratios from immunoblots. Inset: Western blot analysis of Drp-1 in HG, HG+Cur, HG+Rut groups (The experimental group was incubated for 2 h with the addition of the drug.). Error bars, ± s. e. m. n = 3. **p < 0.01 and ***p < 0.001. Bright field image of cell imaging: Figure S28.

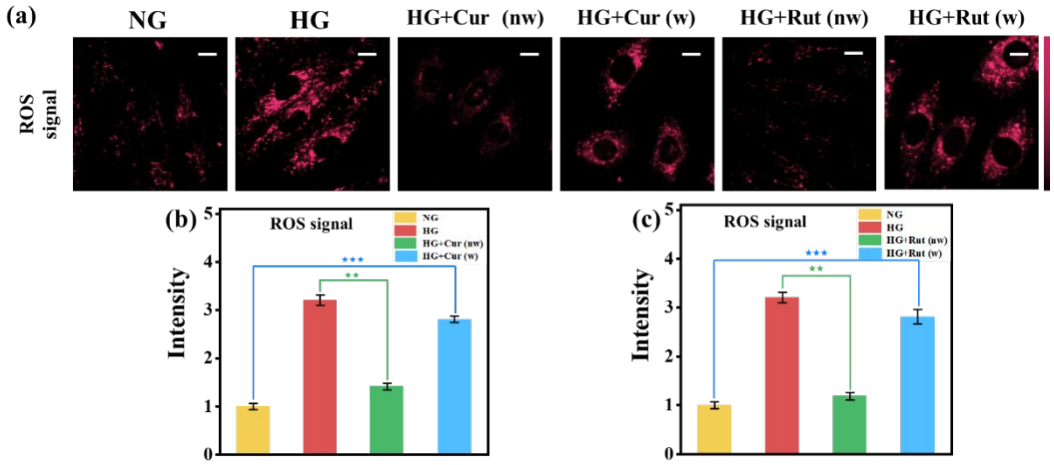

Figure S22. Real-time fluorescence imaging of H9C2 incubated with **HDB** (10 μM). (a) ROS signaling in Figure S20. λ_{am} = 663 - 738 nm, λ_{ex} = 561 nm. Scale bar: 20 μm. (b, c) Normalized average fluorescence intensity of a. As shown in Figure S20 and S21, both the mitophagy signal and ROS signal were inhibited in the no-wash group, while the two signals in the wash-off group were not significant compared with the HG control group, which indicated that Cur and Rut were antioxidant drugs. Meanwhile, western blot analysis also showed that the Drp-1 content was unchanged after adding the drug. Error bars, ± s. e. m. n = 3. **p < 0.01 and ***p < 0.001. Bright field image of cell imaging: Figure S28.

8. MS and ^{1}HNMR

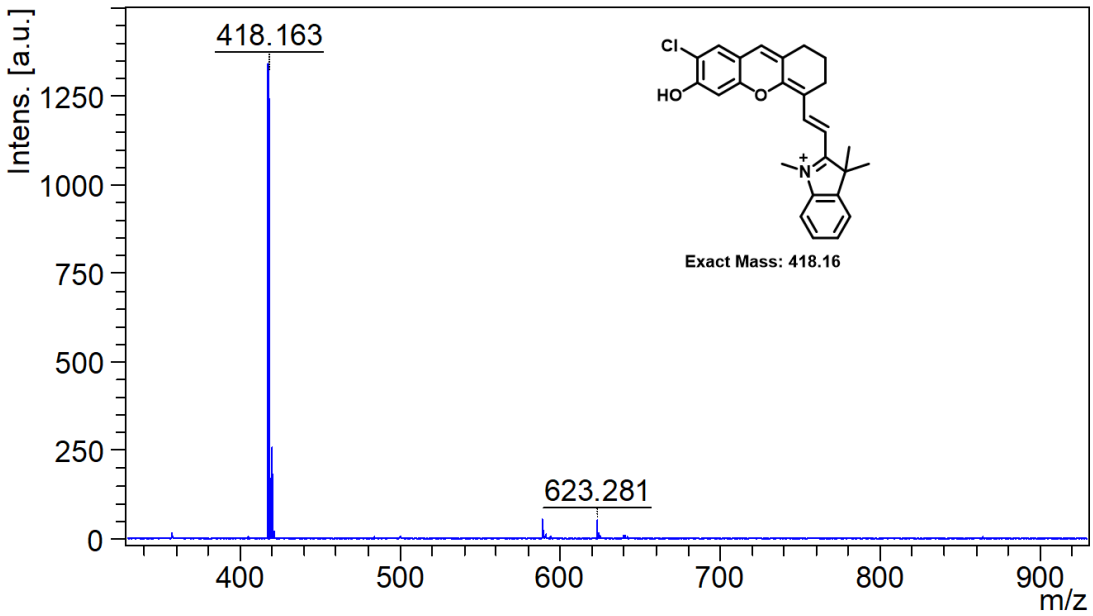

Figure S23. HD-OH MALDI-TOF mass spectrum**.**

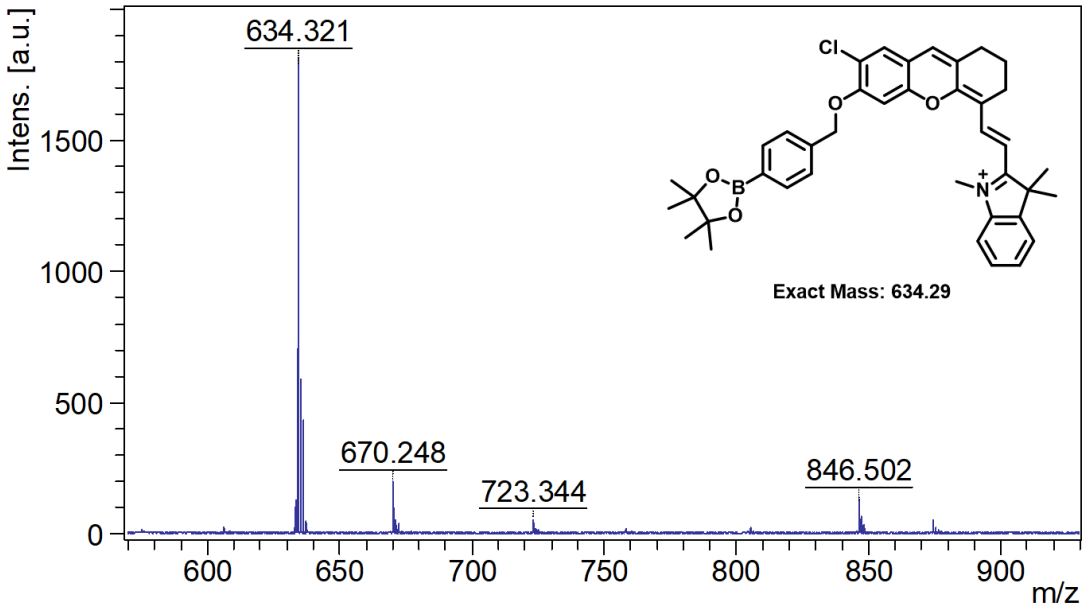

Figure S24. HDB MALDI-TOF mass spectrum**.**

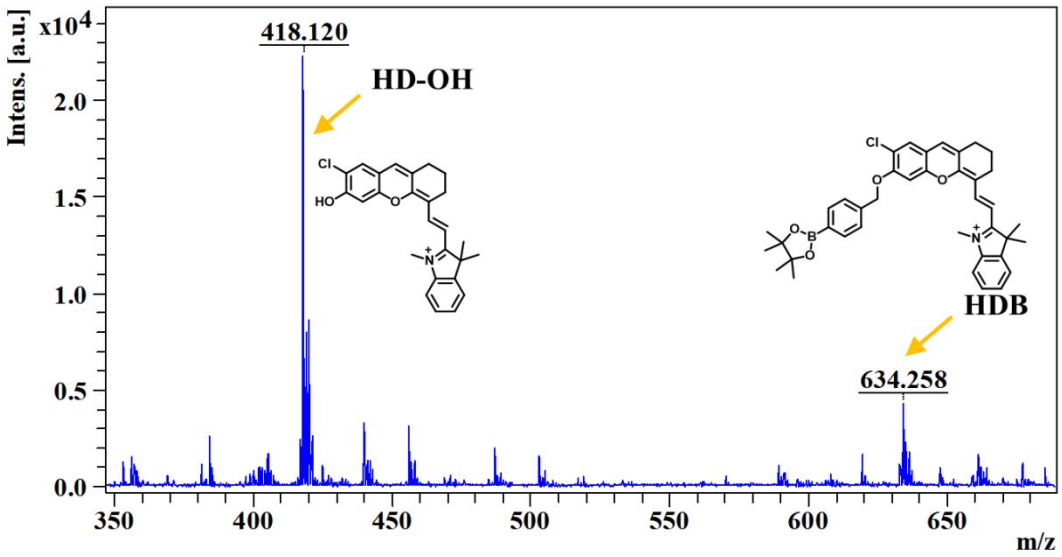

Figure S25. The MALDI-TOF/MS spectrum of **HDB** after response. The mass spectra were characterized after shaking for 30 min at 37 °C when H_2O_2 (300 μM) and **HDB** (5 μM) were added in PBS buffer solution (10 mM, pH = 7.4, PBS: EtOH = 8:2).

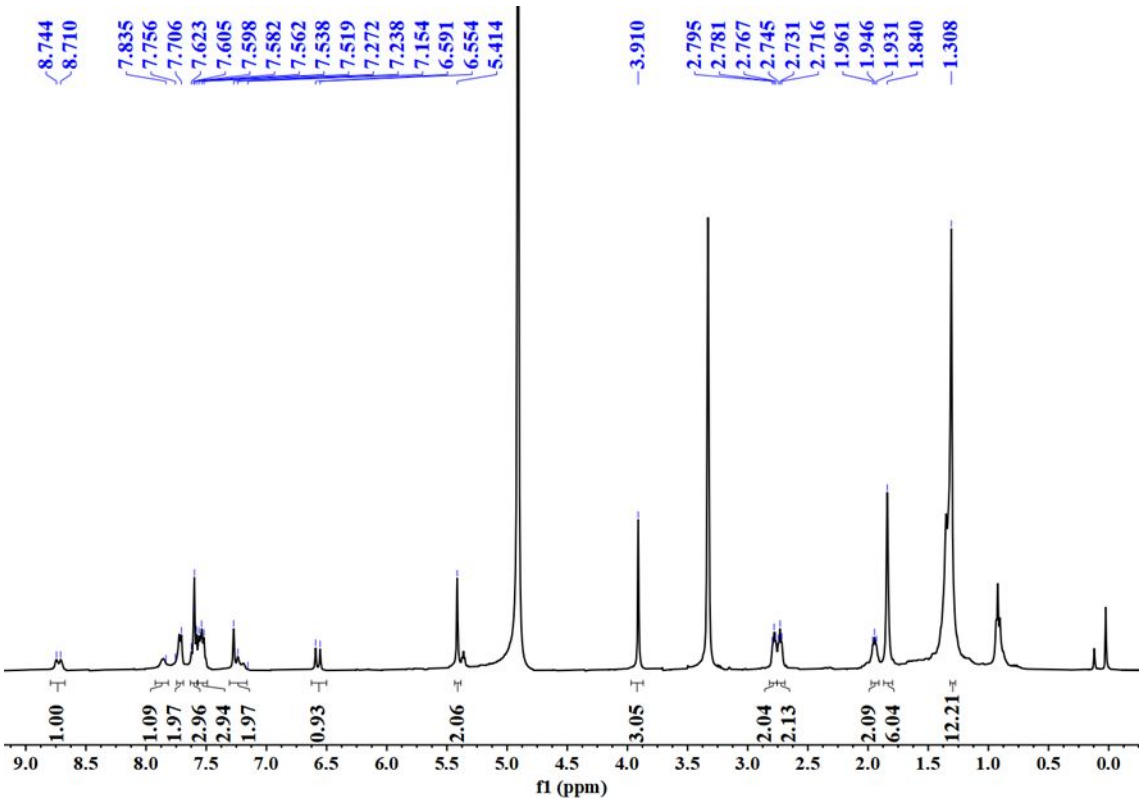

Figure S26. [1]H NMR spectrum of **HDB**.

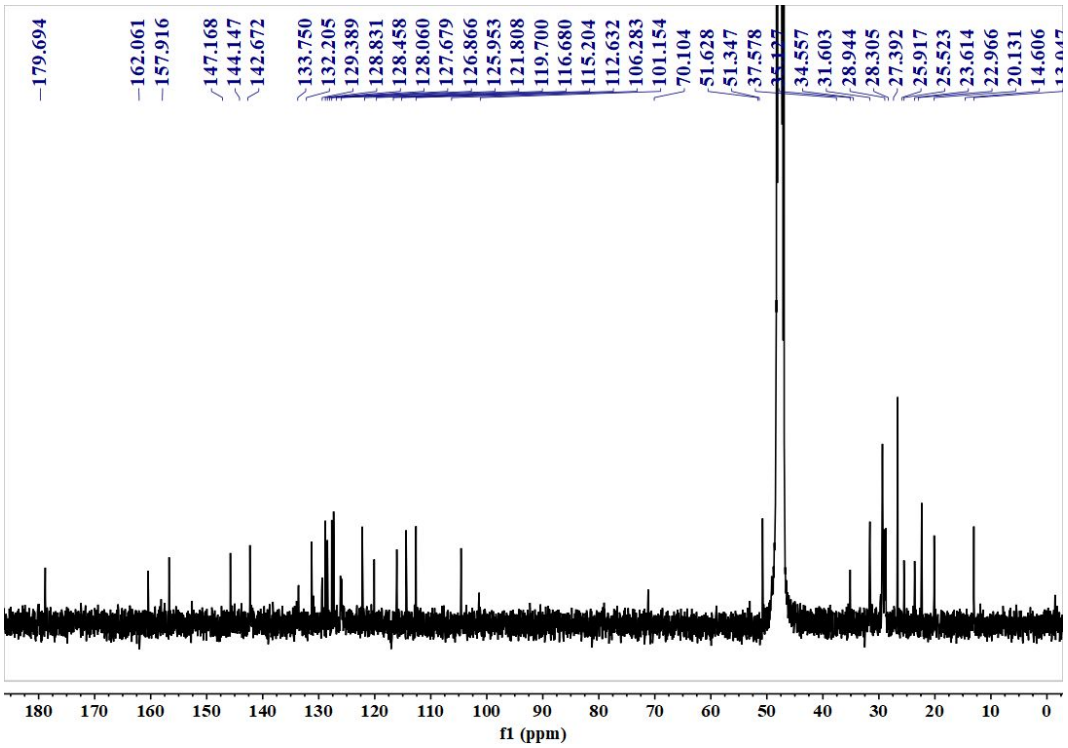

Figure S27. [13] C NMR spectrum of **HDB**.

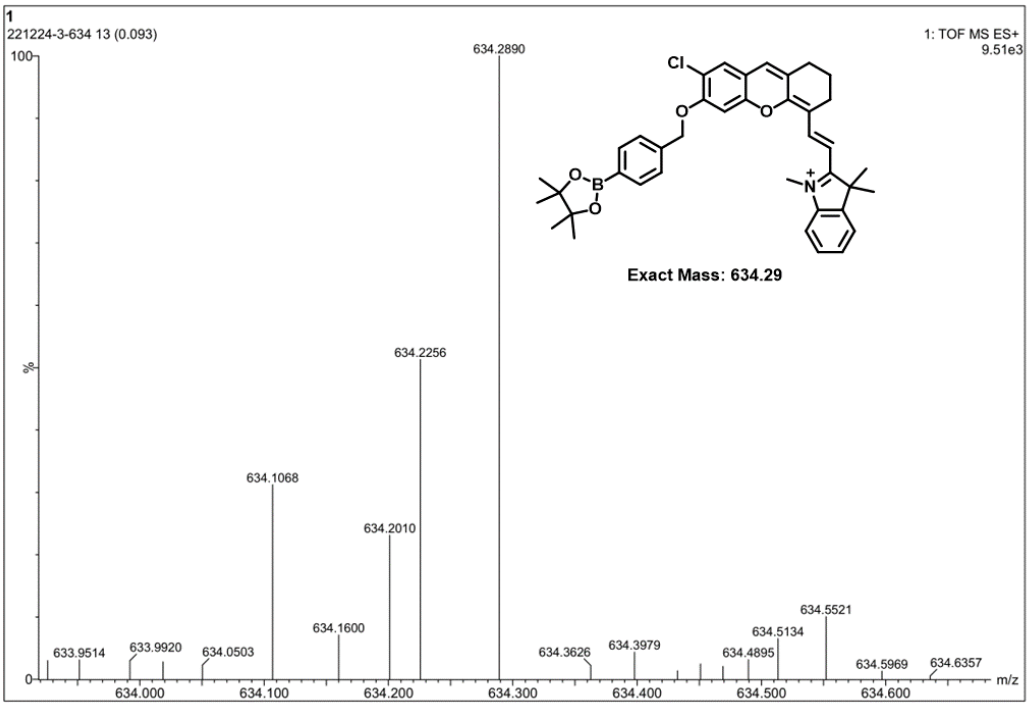

Figure S28. HR-MS spectrum of **HDB**.

9. Cell brightfield image

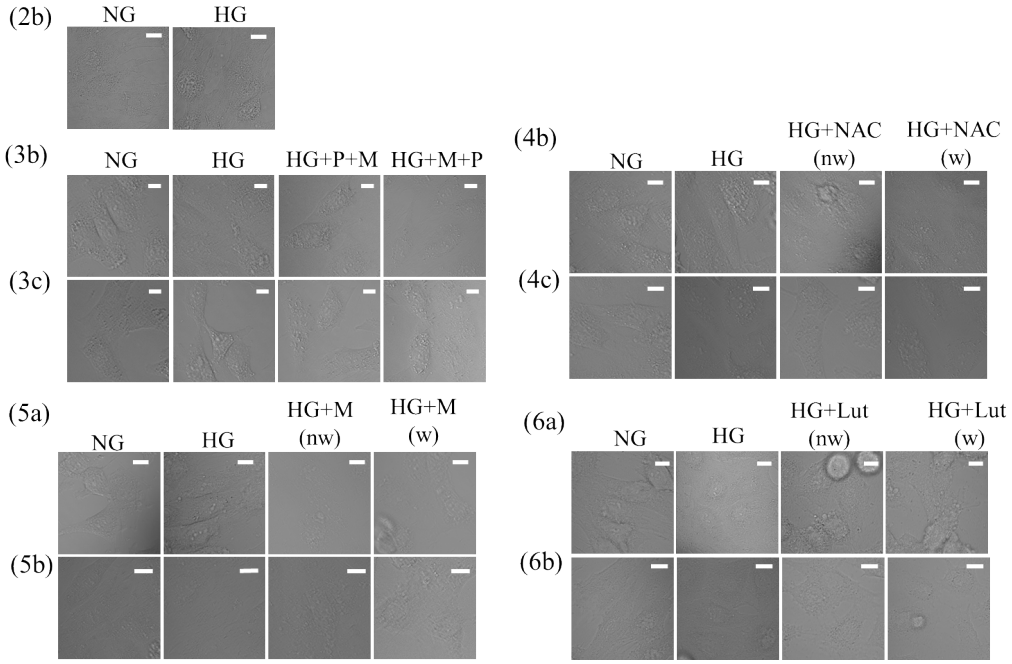

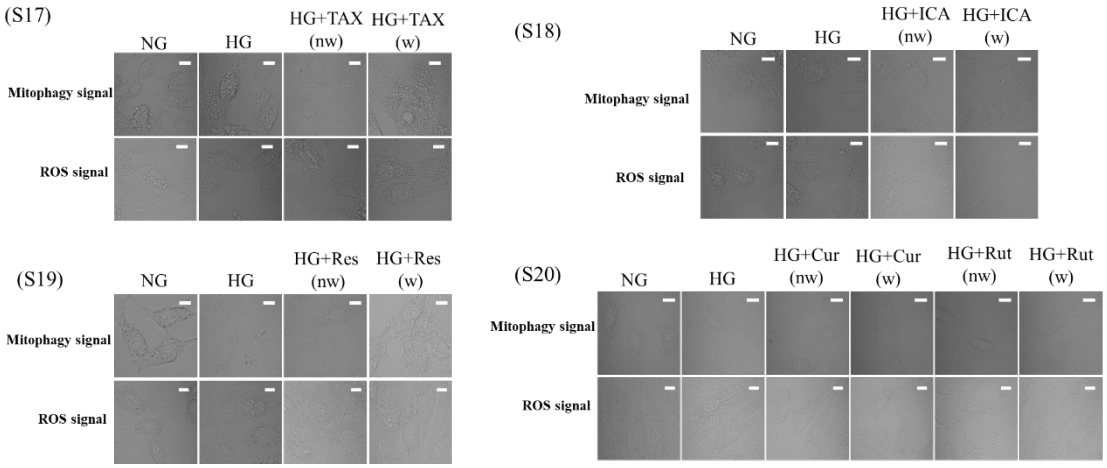

Figure S29. Figure 2, 3, 4, 5, 6, S17, S18, S19, S20 bright field images of the cell imaging.

10. References

(1) Li, Z.; Ren, T. B.; Zhang, X. X.; Xu, S.; Gong, X. Y.; Yang, Y.; Ke, G.; Yuan, L.; Zhang, X. B. Precipitated Fluorophore-Based Probe for Accurate Detection of Mitochondrial Analytes. *Anal. Chem.* **2021**, *93*, 2235-2243. DOI: 10.1021/acs.analchem.0c04094.

(2) Liu, Y.; Teng, L.; Chen, L.; Ma, H.; Liu, H. W.; Zhang, X. B. Engineering of a near-infrared fluorescent probe for real-time simultaneous visualization of intracellular hypoxia and induced mitophagy. *Chem. Sci.* **2018**, *9*, 5347-5353. DOI: 10.1039/c8sc01684d.